Effects of radiofrequency field exposure on proteotoxic-induced and heat-induced HSF1 response in live cells using the bioluminescence resonance energy transfer technique

Emmanuelle Poque, Hermanus J. Ruigrok, Delia Arnaud-Cormos, Denis Habauzit, Yann Chappe, Catherine Martin, Florence Poulletier de Gannes, Annabelle Hurtier, Andre Garenne, Isabelle Lagroye, et al.

Effects of radiofrequency field exposure on proteotoxic- induced and heat-induced HSF1 response in live cells using the Bioluminescence Resonance Energy Transfer technique

Emmanuelle Poque[1*], Hermanus J. Ruigrok[2*], Delia Arnaud-Cormos[3,4], Denis Habauzit[5], Yann Chappe[2], Catherine Martin[5], Florence Poulletier De Gannes[2], Annabelle Hurtier[2], André Garenne[2], Isabelle Lagroye[2,6], Yves Le Dréan[5], Philippe Lévêque[3] & Yann Percherancier[2,§]

[1] Bordeaux University, CNRS, Bordeaux INP, CBMN laboratory, UMR5248, F-33607 Pessac, France
[2] Bordeaux University, CNRS, IMS laboratory, UMR5218, F-33400 Talence, France
[3] Limoges University, CNRS, XLIM, UMR 7252, F-87000 Limoges, France
[4] Institut Universitaire de France (IUF), F-75005 Paris, France
[5] Rennes University, Institut de Recherche en Santé, Environnement et Travail (IRSET) – UMR_S 1085, F-35000 Rennes, France.
[6] Paris Sciences et Lettres Research University, F-75006 Paris, France

* Both authors contributed equally to this work.
§ correspondence to: yann.percherancier@ims-bordeaux.fr

Running Title: Radiofrequency fields' effect on HSF1 activity

ABSTRACT

As of today, only acute effects of RF fields have been confirmed to represent a potential health hazard and they are attributed to non-specific heating (≥1 °C) under high-level exposure. Yet, the possibility that environmental RF impact living matter in the absence of temperature elevation needs further investigation. Since HSF1 is both a thermosensor and the master regulator of heat-shock stress-response in eukaryotes, it remains to assess HSF1 activation in live cells under exposure to low-level RF signals. We thus measured basal, temperature-induced, and chemically-induced HSF1 trimerization, a mandatory step on the cascade of HSF1 activation, under RF exposure to Continuous Wave (CW), Global System for Mobile (GSM), and Wi-Fi modulated 1800 MHz signals, using a Bioluminescence Resonance Energy Transfer technique (BRET) probe. Our results show that, as expected, HSF1 is heat-activated by acute exposure of transiently-transfected HEK293T cells to a CW RF field at a Specific Absorption Rate of 24 W/kg for 30 min. However, we found no evidence of HSF1 activation under the same RF exposure condition when the cell culture medium temperature was fixed. We also found no experimental evidence that, at a fixed temperature, chronic RF exposure for 24 h at a SAR of 1.5 and 6 W/kg altered the potency or the maximal capability of the proteasome inhibitor MG132 to activate HSF1, whatever signal used. We only found that RF exposure to CW signals (1.5 and 6 W/kg) and GSM signals (1.5 W/kg) for 24 h marginally decreased basal HSF1 activity.

Keywords : HSF1, Bioluminescence Resonance Energy Transfer, Radiofrequency, trimerisation.

ABBREVIATION

BRET: Bioluminescence Resonance Energy Transfer
CW: Continuous wave
GSM: Global System for Mobile
Luc: Luciferase
RF: radiofrequency fields.
SAR: Specific Absorption Rate
YFP: Yellow Fluorescent protein
Wi-Fi : Wireless Fidelity

INTRODUCTION

The massive deployment, in our environment, of radiofrequency electromagnetic fields (RF) used for wireless communication systems, raised social concerns about the potential biological and health effects of such radiations. After more than 20 years of researches, the only well-described effect of RF on biological systems is caused by dielectric-relaxation heating. Guidelines and standards have been set to protect from the health risks associated with the thermal effects of RF exposures. In other words, wireless communications emit RF fields that do not induce deleterious tissue heating (Vecchia, 2009). The question remains however open to decipher whether or not RF exposure induces "nonthermal" effects, which ones refer to any potential biological effects that are not caused by the RF-induced increase of temperature in living matter.

In this context, the possibility that environmental RF exposure induces cellular stress responses in various cell types was evaluated considering various biochemical outputs, such as DNA integrity, apoptosis, and protein expression in several human and animal cell cultures (McNamee & Chauhan. 2009; Vecchia, 2009). The "stress proteins", also known as heat-shock proteins (HSPs), are a group of proteins that have been reported to be affected by low-level RF exposures in some studies. Because HSPs and their associated factors are induced by a variety of stressors, they were proposed as possible biomarkers of RF exposure. Articles published before 2012 were reviewed in (McNamee & Chauhan. 2009; Vecchia, 2009; IARC 2013). A limited part of these studies reported altered expression of HSPs in certain cell lines (e.g. (Kwee et al. 2001; Tian et al. 2002; Leszczynski et al. 2002; Miyakoshi et al. 2005; Lixia et al. 2006; Sanchez et al. 2006; Lucas et al. 2007; Ennamany et al. 2008)). Since 2012, eight studies reported increased HSP levels following RF exposure in vitro in PC12 pheochromocytorna cells (Valbonesi et al. 2014), SH-SY5Y neuroblastoma cells (Calabrò et al. 2012), RAW264.7 monocytic cells (Novoselova et al. 2017; López-Furelos et al. 2018), and brain tissue from exposed rats (Yang et al. 2012; Kesari et al. 2014; Sepehrimanesh et al. 2014; López-Furelos et al. 2016). In parallel, four studies reported no RF exposure alteration of HSP level in human corneal cells (Miyakoshi et al. 2019), the brain of young rats (Aït-Aïssa et al. 2013; Watilliaux et al. 2011), and MCF10A human breast epithelial cells (Kim et al. 2012). The majority of these studies measured the expression level of HSP proteins or RNA levels and not all HSP subtypes were tested. From the results, it remains unclear whether these responses were related to specific parameters such as cell line, tissue, frequency, modulation, or were false-positives, e.g. artefacts caused by ill-defined exposure system. Additional well-characterized confirmation studies are required to further evaluate these observations. However, since HSPs activation pathways are driven mainly through protein-protein interaction and phosphorylation cascades, protein-specific approaches may provide more information on the impact of RF on HSP.

The heat shock response is typically characterized by a dramatic upregulation of all heat shock mRNA and proteins level. These biochemical phenomena are induced by heat shock factors (HSF)

such as Heat shock factor 1 (HSF1) which is known as the “master regulator” of heat shock protein transcription in eukaryotes (Gomez-Pastor et al. 2018). During unstressed conditions, molecular chaperones such as Hsp70, Hsp90 and TRiC/CCT interact with HSF1, repressing it by maintaining it inactive in a monomeric form. When the quantity of unfolded proteins increases, i.e. following cellular stress such as a temperature increase, the molecular chaperones bind to the misfolded proteins and dissociate from HSF1. The released HSF1 monomeric proteins undergo homotrimerization, which renders it transcriptionally active. The full activation of HSF1 trimers is also regulated by several posttranslational modifications such as phosphorylation and sumoylation. Active HSF1 trimers will accumulate into the nucleus where they bind to its DNA-responsive element, named HSE for heat shock element. These DNA sequences are found in upstream regulatory regions of *HSP* genes and *HSF* genes themselves (Dayalan Naidu & Dinkova-Kostova. 2017). Therefore, assessing HSF1 activation level in cells allows monitoring of the RF effects on the HSP-driven cellular stress response in an integrated way.

For the last twenty years, techniques based on the non-radiative transfer of energy between an energy donor and a compatible fluorescent energy acceptor emerged as powerful techniques for measuring in real-time the activity of an impressive array of proteins in live cells (Miyawaki & Niino. 2015). The key point of these techniques is the absolute reliance of the energy transfer efficiency to the molecular closeness (around 10 nm) and orientation between donor and acceptor dipoles. Thanks to these properties, RET techniques allow monitoring of both constitutive and regulated inter- and intra-molecular interactions. Based on RET techniques, we have recently demonstrated that Bioluminescence Resonance Energy Transfer (BRET) is useful for measuring proteins interactions and conformational changes in real-time and in live cells under RF exposure (Ruigrok et al. 2018; Poque et al. 2020). The present study aimed at evaluating the potential effects of 1800 MHz RF signals on HSF1 activation in live cells using a BRET-based molecular probe. We constructed and characterized an efficient HSF1 intermolecular BRET probe with which we monitored basal, temperature-induced, and chemically-induced HSF1 activity in live human HEK293T cells exposed under isothermal conditions to various signals. Specific Absorption Rate (SAR) levels of 1.5 and 6 W/kg were applied with 1800 MHz RF of Continuous Wave (CW) or Global System for Mobile (GSM)-, and WiFi-modulated signals.

MATERIAL AND METHODS

Plasmids

To generate the BRET constructs, super Yellow Fluorescent Protein 2 (Kremers et al. 2006) and Renilla Luciferase II (Loening et al. 2006) were used to improve the brightness of the assay. They are referred as YFP and Luc in the rest of the manuscript. The human full-length *HSF1* cDNA was a gift from Dr. NF. Mivachi (Center for Molecular Chaperone Radiobiology & Cancer Virology Group, Augusta University, GA, USA). The HSP90 expression vector was obtained by subcloning the human HSP90AA1 cDNA from the pCR-BluntII-TOPO-HSP90AA1 vector (Harvard Medical School PlasmID Repository, clone HsCD00347538) as BamH1-XhoI PCR fragment in the multi-cloning site of the vector pcDNA3.1 using the primers "hHSP90_BamHI_ATG_Sense" (TGTCTGGTACCGGATCCGCCACCATGCCTGAGGAAACCCAGACCCAAGACC) and "hHSP90_Stop_XhoI_antisense" (ATCTAGTCTAGACTCGAGCGGTTAGTCTACTTCTTCCATGCGTGATGTGTCG). The Luc-hHSF1 expression vector was obtained by subcloning the cDNA of h*HSF1* as an EcoRI-XbaI PCR fragment in place of the YFP in the EcoRI-XbaI site of the pcDNA3.1 Luc-YFP vector described in (Ruigrok et al. 2017). Using a similar strategy, the YFP-HSF1 expression vector was obtained by replacing Luc cDNA by the one coding hHSF1 in the EcoRI-XbaI site of the pcDNA3.1 YFP-Luc vector described in (Ruigrok et al. 2017). In both case, h*HSF1* cDNA was amplified by PCR using the "Fus_EcoRI_hHSF1_Sense" primer (TGTGTACCGGTGAATTCTGGTGGAGGCGGATCTATGGATCTGCCCGTGGGCCCCGGCG) and the "hHSF1-STOP-XbaI" primer (ATCTAGTCTAGACTCGAGCGGTTAGGAGACAGTGGGGTCCTTGGCTTTGG). For all configurations, the sequence joining Luc or YFP sequence to h*HSF1* encodes VPVNSGGGGS as a linker. The sequence of each cDNA construct was confirmed by DNA sequencing.

Reagents

MG132 and Thapsigargin were from Sigma (Lyon, France). Coelenterazine H and Purple Coelenterazine (Nanolight Technology, Pinetop, AZ, USA) were added to a final concentration of 5 µM. Anti-β-actin (sc-8432) and anti-HSF (sc-17756) antibodies were purchased from Santa Cruz Biotechnology (Dallas, TX, USA). Anti-Hsp70 (SPA801) and anti-BIP (AB21685) antibodies were obtained from Stressgen (San Diego, CA, USA) and Abcam (Cambridge, UK) respectively.

Cell culture and transfections

HEK293T cells were maintained in Dulbecco's modified Eagle's medium – high Glucose (DMEM) (D6429, Sigma) supplemented with 10 % fetal bovine serum, 100 units mL-1 penicillin and

streptomycin. Twenty-four hours before transfection, cells were seeded at a density of 500,000 cells per well in 6-well dishes. Transient transfections were performed using polyethylenimine (PEI, linear, Mr 25,000; catalogue number 23966 Polysciences, Inc., Warrington, PA, USA) with a PEI:DNA ratio of 4:1, as explained in (Percherancier et al. 2005). For all experiments, 0.1 µg of Luc-HSF1 expression vector was co-transfected with 1.4 µg of YFP-HSF1 and 0.5 µg of HSP90 expression vectors. After overnight incubation, transfected cells were then detached, resuspended in DMEM w/o red phenol (Ref 21063-029, ThermoFisher scientific, Waltham, MA, USA) and replated at a density of 10^5 cells per well in 96-well white plates with clear bottoms (Greiner Bio one, Courtaboeuf, France) pre-treated with D-polylysine (Sigma) for reading with the Tristar2 luminometer (Berthold Technologies, Bad Wildbad, Germany) or onto 12 mm diameter glass coverslips (Knittel Glass, Braunschweig, Germany) treated with D-polylysine for the reading with the SpectraPro 2300i spectrometer (Acton Optics, Acton, MA, USA) (see below). Cells were left in culture for 24 h before being processed for the BRET assay.

Emission spectra and BRET assays

The experimental emission spectra of Luc-HSF1 (with coelenterazine H), and YFP-HSF1 were first obtained experimentally using a Cary Eclipse Fluorimeter (Agilent Technologies, Santa Clara, CA, USA) to assess the functionality of the Luc and YFP groups fused to HSF1 (Fig. S1).

BRET signals were acquired either in real time under acute RF exposure, as described in (Ruigrok et al. 2018), or following RF exposure for 24h at SARs close to environmental levels, as described in (Poque et al. 2020). In all cases, the BRET signal was determined by calculating the ratio of the light intensity emitted by the YFP (energy acceptor) over the light intensity emitted by the Luc (energy donor) according to Eq.1:

(1): $$BRET = \frac{I_{acceptor}}{I_{donor}}$$

When the BRET signals were measured in real time under RF exposure, full BRET spectra were acquired using an optical fiber linked to a Spectra Pro 2300i spectrometer (Princeton Instruments, Acton, MA, USA) equipped with a liquid-nitrogen-cooled charge-coupled device camera for recording the full visible spectrum (Acton Optics). In that case, since we were able to fully differenciate the Luc spectra from the YFP spectra using real-time spectral decomposition, $I_{acceptor}$ and I_{donor} were calculated by integrating the area under the curves of the acceptor and the donor spectra. The BRET signal was presented as the Net BRET (Ruigrok, 2017). Under that configuration, glass coverslips containing the cells were placed into a white opaque measurement chamber made of Teflon and containing 1.5 mL of saline solution (NaCl 0.145 M, KCl 5 mM, KH_2PO_4 4 mM, $CaCl_2$ 1 mM, $MgSO_4$ 1 mM, Glucose 10 mM) (Ruigrok et al. 2018). Coelenterazine H was added to the cells and full BRET spectra were acquired every 3 s and analyzed as explained in (Ruigrok et al. 2017).

To measure BRET signals after RF chronic exposures, transfected HEK293T cells seeded in 96-well plates were exposed for 24 hours to the indicated RF exposure conditions, with the last 12 hours being in presence or absence (sham) of various concentrations of MG132. Coelenterazine H was then added to the cell culture medium at a final concentration of 5 µM and BRET assays were immediately performed using a multidetector TriStar2 LB942 microplate reader (Berthold Technologies, Bad Wildbad, Germany) and emission filters centered at 540 ± 40 nm for YFP ($I_{acceptor}$) and 480 ± 20 nm for Luc (I_{donor}). Due to the overlapping emission spectra of Luc and YFP, a fraction of the light detected in the YFP filter originates from the Luc emission, resulting in a contaminating signal (Hamdan et al. 2006). In that configuration, the Net BRET was therefore defined as the BRET ratio of cells co-expressing Luc and YFP constructs minus the BRET ratio of cells expressing only the Luc construct in the same experiment.

Western-blot analysis

Cells were scraped from the culture plate by using Laemmli extraction buffer. Proteins were then separated on a 7.5% (w/v) polyacrylamide denaturing gel and transferred onto a nitrocellulose membrane (Amersham Biosciences, Buckinghamshire, UK). Western blotting was performed as previously described (Loison et al. 2006). Primary antibodies were revealed using horseradish peroxidase-conjugated IgG (Amersham ECL), followed by chemiluminescence detection as recommended by the manufacturer's instructions (Merck KGaA, Darmstadt, Germany).

RF field exposure system

The RF exposure system was a tri-plate open transverse electromagnetic (TEM) cell allowing RF signals propagation (Ruigrok et al. 2017). A vector generator (SMBV100A, Rohde & Schwarz, Munich, Germany) connected to a 10 W preamplifier and a 200 W amplifier (RF14002600-10, and RFS1800-200, RFPA, Artigues-Près-Bordeaux, France) with around 40- and 8-dB gain, respectively, were used to deliver 1800 MHz RF signals to the exposure system.

To assess the effect of acute RF effect on HSF1, HEK293T cells were exposed to RF in a Teflon chamber containing 1.5 mL of medium placed on the lower ground plate of the TEM cell, as described in (Ruigrok et al. 2018). The cell culture medium temperature was regulated using a Thermostat Plus microplate Peltier heater (Eppendorf, Hamburg, Germany) placed under the TEM cell and monitored using a fiber optic temperature probe (Luxtron-812, Lumasense Technologies, Santa Clara, USA). Temperatures and BRET data were simultaneously recorded in real time as described in (Ruigrok et al. 2017).

To measure the effect of RF chronic co-exposure with MG132 on HSF1 activity, HEK293T cells were exposed for 24h in a 96-well plate containing 200 µL of medium, as described in (Poque et

al. 2020). Investigations were carried out at two SAR levels using three 1800 MHz RF signals (CW, GSM, and Wi-Fi- modulated signals).

RF Dosimetry

The characterized exposure system was a TEM cell containing a Teflon chamber for acute exposures or a 96-well plate for chronic exposures. Numerical dosimetry of the exposure system was performed using in-house Finite Difference Time Domain (FDTD)-based software for solving Maxwell's differential equations. Details of the numerical dosimetry can be found for the Teflon chamber in (Ruigrok et al. 2018) and for the 96-well plate in (Poque et al. 2020).

The incident power was adjusted to apply the same average power level for all signals at 1800 MHz. For the Teflon chamber, based on the SAR efficiency (5.2±1.9 W/kg/W, mean±SD) computed in (Ruigrok et al. 2018), the incident powers applied in this study were set to obtain two SAR levels. For the 96-well plate, the volume of medium was different from (Poque et al. 2020) where each well was filled with 100 µL. The dosimetry was thus carried out in this study with a 96-well plate containing 200 µL of medium and the SAR efficiency was 0.69±0.07 W/kg/W. The SAR values within the cells layer were 6.2±1.4 and 0.90±0.09 W/kg/W, for the Teflon chamber and for the 96-well plate, respectively. The two exposure levels for the whole-volume mean SAR values were 1.5 and 6.0 W/kg. Experimental dosimetry was carried out using a fiber optic temperature measurement system (Luxtron 812, LumaSense Technologies, Erstein, France.) for temperature measurements inside the Teflon chamber and inside several wells, containing 200 µL of medium, of the 96-well plate. SAR assessment from temperature measurements was described in details in (Ruigrok et al. 2018). SAR values obtained from numerical simulations and experimental measurements are in good agreement. Table 1 presents the power settings at the vector generator to obtain the required SAR values for all signals. The averaged output power delivered by the signal generator was measured using a power meter and a wideband power sensor (N1912A and N1921A, Agilent, Santa Rosa, CA, USA).

Table 1: Vector Generator Power Levels Settings for the three signals, two SAR levels and two exposure configurations.

SAR	Vector Generator Power Levels Settings (dBm)					
	Teflon chamber*			96-well plate**		
	CW	GSM	WiFi	CW	GSM	WiFi
1.5 W/kg	–23.1	–15.1	–23.5	–6.89	1.11	–7.34
6.0 W/kg	–17.1	–9.1	–17.5	–0.89	7.13	–1.34
24.0 W/kg	–11.1			Not tested		

*47.7 dB amplifier gain

**40.6 dB amplifier gain

Statistical analysis

GraphPad Prism v6.00 for Windows (GraphPad Software, La Jolla, CA, USA) was used for plotting dose-response curves. Statistical analyses were performed using Anastats (Rilly sur Vienne, France). The one sample Wilcoxon signed-rank test was used to assess the statistical significance against the null hypothesis of the difference calculated between Sham and RF exposure condition for basal BRET, MG132 potency and efficacy. P-values less than 0.05 were considered as statistically significant.

RESULTS

To build a BRET probe that can efficiently measure HSF1 activity in live cells, we took advantage of the required trimerisation step on the roadmap of HSF1 activation. We constructed the cDNA coding for N-terminally Luc- and YFP-tagged HSF1 (respectively Luc-HSF1 and YFP-HSF1). This approach was based on the hypothesis that if HSF1 proteins tagged with a bioluminescent energy donor are co-expressed in a cell with HSF1 proteins tagged with a fluorescent energy acceptor, the resulting BRET signal might increase following HSF1 activation since trimerization brings donor and acceptor groups in close proximity (Fig. 1).

HSF1 activation is triggered by heat (Zou et al. 1998; Hentze et al. 2016). The effect of temperature elevation on the BRET spectra measured from HEK293T cells transiently transfected with Luc-HSF1 and YFP-HSF1 was first assessed. As shown in Fig. 2A, a resonance energy transfer occurs at 25 °C between YFP-HSF1 and Luc-HSF1 since a light peak with a maximum emission at 535 nm corresponding to the acceptor reemission can be detected in addition to the Luciferase light emission that peaks at 485 nm, in agreement with the individual emission spectra of both Luc-HSF1 and YFP-HSF1 (Fig. S1). This basal energy transfer observed indicates that some HSF1 constitutive oligomers already exist in resting conditions under our experimental conditions. As expected, increasing the temperature to 45 °C for 5 min led to the increase in the amount of light emitted in the 510 –550 nm region that resulted from the transfer of energy from the luciferase to the YFP with the ensuing emission of light by the latter (Fig. 2A). To further characterize the temperature sensitivity of our HSF1-based intermolecular BRET probe, the BRET signal, defined as the ratio of light detected for YFP over the light detected for Luc (see material and methods for details), was then measured in real time while heating the cell culture from 22 to 48 °C using a Peltier heater (Fig. 2B). The initial basal BRET signal remained stable between 22 and 35 °C. It then linearly increased with the temperature and reached a short plateau between 44 and 46°C, before slightly decreasing between 46 and 48°C. This result indicates that, under our experimental conditions, HSF1 is activated by heat with a threshold around 35 °C and a maximum activation is reached for temperatures above 40 °C as previously observed (Zou et al. 1998; Hentze et al. 2016).

To further characterize the Luc-HSF1/YFP-HSF1 intermolecular BRET test, we assessed its sensitivity to MG132-induced proteotoxic stress. MG132 is a well-known proteasome inhibitor that has been shown to induce HSF1 activation by increasing cytosolic misfolded protein content (Mathew et al. 2001). As expected, MG132-induced a dose dependent increase of the BRET signal with a 3-fold maximal increase of the basal BRET signal and an EC50 in the hundred nanomolar range (pEC50 = 6.61±0.06, Fig. 3A). As control, we verified by western blot that overnight treatment with 5 µM MG132 induced overexpression of HSP70. This increase could be measured in both un-transfected and transfected cells (Fig. 3B) confirming that MG132 treatment was effective in activating HSF1, as previously described (Mathew et al. 2001). However, under our condition (concentration and duration

of treatment), MG132 did not produce any change in the expression level of Bip1 (also known as GRP78), a well known ER stress marker, which is activated by the ER stress-related factor ATF6 but not by HSF1 (Lee. 2005). Both mock-transfected HEK293T cells and HEK293T cells co-expressing Luc-HSF1 / YFP-HSF1 proteins were incubated overnight with increasing concentrations of Thapsigargin. Addition of Thapsigargin, which is a well-known competitive inhibitor of the sarco/endoplasmic reticulum Calcium ATPase (SERCA), leads to emptying the intracellular calcium stores (Burnay et al. 1994) and the subsequent triggering of endoplasmic reticulum stress following prolonged exposure (Li et al. 1993). Overnight treatment with 10 nM Thapsigargin efficiently induced an ER stress as shown by the increase in BiP protein expression level (Fig. 3B). However, even at high Thapsigargin concentrations, we could only measure a low BRET increase between Luc-HSF1 and YFP-HSF1 (Fig. 3A). Similar results were obtained in Huh-7 hepatocarcinoma cell line, further reinforcing these observations (Fig. S2).

Altogether, these results indicate that the BRETsignal measured with our intermolecular BRET assay is specific of HSF1 activation by heat or proteasome inhibition.

HEK293T cells expressing Luc-HSF1 / YFP-HSF1 BRET probes were then exposed to a CW 1800 MHz RF signal at an initial temperature slightly above 35 °C that corresponds to the measured HSF1 heat activation threshold. Temperature of the cell medium and BRET signal were simultaneously recorded before and during RF exposure. Immediately after the onset of RF exposure, an increase in BRET signal was observed indicating that HSF1 was activated due to RF-induced temperature elevation (Fig. 4A). A final temperature increase of 3.5 °C was observed under exposure at a whole volume SAR around 24 W/kg for 30 min (Fig. 4B). Such RF-induced temperature increase may have masked the potential nonthermal HSF1 activation by RF exposure. In order to unravel the nonthermal HSF1 activation during RF exposure, the cell culture medium temperature was clamped using a Peltier plate. Clamping the cell-culture medium at ca. 36 °C abrogated the rise of the BRET signal which stayed stable during exposure to RF at 24 W/kg (Fig. 4A and B). The resulting BRET signal was similar with the no-RF control condition indicating that HSF1 was not activated by RF exposure at steady temperature.

The effect of RF co-exposure with MG132 on HSF1 activity was further assessed. Cells in a culture medium at 37 °C were exposed during 24 h to 1800 MHz CW, GSM or WiFi signals at two different SAR values of 1.5 W/kg and 6 W/kg. In this configuration, HEK293T cells transfected with the HSF1 BRET probe were pre-exposed to RF for 12 hours before being co-exposed for another 12 h with RF and increasing doses of MG132. Analysis of the resulting dose-response curves (Fig. 5A-F) indicates that the basal BRET ratio of the intermolecular BRET probe Luc-HSF1 / YFP-HSF1 is slightly but reproducibly decreased, in comparison to the sham control, when cells were exposed to CW and GSM signals at 1.5 W/kg (Fig. 5G). However, the basal BRET signal was not modified when cells were exposed to CW and GSM signals at 6 W/kg SAR or exposed to WiFi signal at either 1.5 or

6 W/kg. For all signals or SAR values, RF exposure did not modify MG132 potency to activate HSF1 (Fig. 5H). However, a slight but statistically significant increase of the MG132 maximal efficacy to activate HSF1 was measured (fig. 5I). This increase was 5% for exposures to the CW signal at 1.5 and 6 W/kg and 7% for GSM at 1.5 W/kg in comparison to the sham control for each condition. No RF exposure effect was detected on MG132 maximal efficacy to activate HSF for exposures to GSM at 6 W/kg or to WiFi signal whatever SAR used.

DISCUSSION

Few studies have addressed the effect of RF on HSF1 levels and/or activity. In a very comprehensive study, Ohtani et al (2016) assessed the changes in the expression of Hsp and Hsf families in the cerebral cortex and cerebellum of Sprague-Dawley rats. The animals were exposed for 3 or 6 h/day to 2.14 GHz wideband code-division-multiple-access (W-CDMA) RF signals at a whole-body averaged specific SAR of 4 W/kg (Ohtani et al. 2016). These authors found that RF exposure at 0.4 W/kg, which is the limit for the occupational exposure set by the International Commission on Non-Ionizing Radiation Protection, caused behavioral disruption in the laboratory animals. Transcriptional analyses revealed a significant upregulation of some of the *Hsp* and *Hsf* genes, particularly in the cerebellum, for rats that were exposed to 4 W/kg for 6 h/day. No changes were measured at 0.4 W/kg or if rats were exposed at 4 W/kg for only 3 h/day. This effect was associated with an increase in core temperature by 1.0-1.5 °C with respect to the baseline, indicating a possible thermal effect of RF on hsf and hsp gene expression. In the study by Laszlo et al. (2005), the DNA-binding activity of HSF in the hamster, mouse and human cells was determined. Acute and continuous exposures to 835.6 MHz 'frequency domain multiple access' (FDMA)- or 847.7 MHz 'code domain multiple access' (CDMA)-modulated RF at two SAR values (0.6 and ca. 5 W/kg) were studied (Laszlo et al. 2005). Under all exposure conditions, the authors reported a lack of HSF DNA-binding ability induction in cultured mammalian cells. The only studies showing a slight effect of RF exposure on HSF gene activity and heat-shock response had been performed in the nematode *C. elegans* (de Pomerai et al. 2000; de Pomerai et al. 2003). This effect has since been reinterpreted as a subtle thermal artefact caused by small temperature disparities (≤0.2 °C) between exposed and sham conditions (Dawe et al. 2006).

In the present study, we designed and characterized an intermolecular BRET assay measuring HSF1 activation through the assessment of its trimerisation in real-time and live cells. This assay responded specifically to both MG132-induced proteotoxic stress known to trigger HSF1 activation and heat activation with thresholds similar to those reported in the literature (Fig. 2 and 3). Using this BRET probe, we monitored HSF1 activation under RF exposure, CW, GSM- or WiFi-modulated signals at 1800 MHz and SAR levels of 1.5 and 6 W/kg (24 h chronic exposure) or 24 W/kg for CW (acute exposure). As expected, HSF1 was activated under RF-exposure-associated temperature elevation. To exclude specific non-thermal effects of RF, exposures at a constant temperature of 36 °C were performed under RF exposure. There were no effects of acute RF exposure on the activation state of HSF1 at a steady temperature (Fig. 4). This observation was consistent with previous experiments, showing that HSF-sensitive reporter genes were not activated under non-thermic electromagnetic exposure (Zhadobov et al. 2007). At constant temperature, we tested the chemical mode of HSF1 activation using MG132. We found that RF exposure to CW signals (1.5 and 6 W/kg) and GSM signal (1.5 W/kg) only marginally increased MG132 maximal efficacy (5-7 % increase in maximal efficacy

compared to the sham condition) and did not modify MG132 potency to activate HSF1 (Fig. 5). For both CW and GSM exposures at 1.5 W/kg, the slight increase in MG132 maximal efficacy correlated with a concomitant slight decrease in HSF1 basal BRET and an identical HSF1 maximal BRET level in saturated MG132 concentration. This indicates that RF slightly decreased HSF1 basal activation state without affecting the maximal capability of HSF1 to be activated under proteotoxic stress conditions. No effects were observed in GSM-modulated 1800 MHz RF exposures at 6 W/kg for 24 h on basal HSF1 activity, MG132 efficacy and potency to activate HSF1. The same observation applied for 1800 MHz Wi-Fi signals. The minor decrease in HSF1 basal activity measured after RF exposure for 24 h at 1.5 W/kg using CW and GSM signals was inconsistent among the various signals/SAR values tested. Also, MG132 maximal efficacy to stimulate HSF1 activity was increased following 24 hr exposure to CW or GSM signals at 1.5 W/kg and CW signal at 6 W/kg. In conclusion, our study showed (i) no evidence that RF exposures under isothermal conditions affect HSF1-trimerisation and activation in response to proteotoxic or thermal stress, and (ii) evidence that HSF1 basal activation state might be slightly modified by RF exposure. Altogether, our results indicate that RF exposure at an environmental level or in isothermal condition does not impact HSF1 activation capability.

The future deployment of the fifth-generation (5G) wireless communication will boost the rise of the Internet of Things. The consequence will be a massive increase in the number of high-frequency-powered base stations and other wireless devices everywhere in our environment. Such technologies will use carriers waves in the 3.5-5.5 and 26 GHz bands. It is important to point here that the dielectric loss of water peaks around 26 GHz at body temperature (Buchner et al. 1999). This implies that RF energy will not penetrate the body as it will be absorbed by the first layer of the body with very high efficacy. At 26 GHz, the main issues to be studied in bioelectromagnetics studies become dermis and eyes. As a consequence, it will be of prime importance to assess the potential stress response induced by 5G signals in particular in these tissues using our HSF1 intermolecular BRET probes.

Beyond the scope of bioelectromagnetics, HSF1 has been validated as a powerful target and biomarker in cancer since a broad spectrum of cancer cells exhibit high levels of nuclear-active HSF1 (Carpenter et al. 2019). Since HSF1 protects cells from stresses induced by chemicals, radiation, and temperature, this high level of nuclear-active HSF1 is detrimental for cancer therapies such as radiation, chemotherapy and hyperthermia (Tabuchi et al. 2013; Dong et al. 2019). Inhibiting HSF1 in cancer cells is therefore promising to improve cancer treatment, but this intrinsically depends on the ability to discover drugs that specifically target HSF1. All existing cell-based approaches for HSF1 activity identify molecules that inhibit general transcription, translation, or upstream signaling processes and are predicted to have more ‘off-target’ effects. By targeting the HSF1 trimerization interface in live cell and in real time, the herein presented BRET assay can contribute to improving HSF1 drug screening. Concomitantly, HSF1 intermolecular BRET probe my also be very useful to

assess the stress response induced in healthy tissue in a number of medical application techniques devoted or not to cancer treatment.

Declarations

FUNDING SOURCE

The research leading to these results received funding from the European Community's Seventh Framework Programme (FP7/2007-2013) under grant agreement no. 603794 (the GERONIMO project).

DECLARATION OF INTEREST

The authors declare no competing interests.

ETHICS APPROVAL

Not applicable

CONSENT TO PARTICIPATE

Not applicable

CONSENT FOR PUBLICATION

Not applicable

AVAILABILITY OF DATA AND MATERIAL

Data available on request from YP (mail: yann.percherancier@ims-bordeaux.fr).

CODE AVAILABILITY

Not applicable

AUTHORS' CONTRIBUTIONS

YP conceived and designed the study. PL and DAC designed the device and performed the electromagnetic dosimetry. EP, LP, HJR, FPDG, AH, RR, DH, CM, YLD and YP collected and assembled the data. AG performed the statistical analysis of the results. YP, IL, YLD, DAC and PL wrote the manuscript. All co-authors read and approved the final manuscript.

ACKNOWLEDGMENTS

We thank Bernard Veyret for his wise advice and proofreading of the manuscript.

REFERENCES

Aït-Aïssa S, de Gannes FP, Taxile M, Billaudel B, Hurtier A, Haro E, Ruffié G, Athané A, Veyret B, Lagroye I (2013) In situ expression of heat-shock proteins and 3-nitrotyrosine in brains of young rats exposed to a WiFi signal in utero and in early life. Radiat Res 179:707-716. https://doi.org/10.1667/RR2995.1

Buchner, R, J Barthel, J Stauber (1999) The Dielectric Relaxation of Water Between 0°C and 35°C. Chemical Physics Letters 306:57-63. https://doi.org/10.1016/S0009-2614(99)00455-8

Burnay MM, Python CP, Vallotton MB, Capponi AM, Rossier MF (1994) Role of the capacitative calcium influx in the activation of steroidogenesis by angiotensin-II in adrenal glomerulosa cells. Endocrinology 135:751-758. https://doi.org/10.1210/endo.135.2.8033823

Calabrò E, Condello S, Currò M, Ferlazzo N, Caccamo D, Magazù S, Ientile R (2012) Modulation of heat shock protein response in SH-SY5Y by mobile phone microwaves. World J Biol Chem 3:34-40. https://doi.org/10.4331/wjbc.v3.i2.34

Carpenter, Richard L, Yesim Gökmen-Polar (2019) HSF1 As a Cancer Biomarker and Therapeutic Target. Current cancer drug targets 19:515-524. https://doi.org/10.2174/1568009618666181018162117

Dawe AS, Smith B, Thomas DW, Greedy S, Vasic N, Gregory A, Loader B, de Pomerai DI (2006) A small temperature rise may contribute towards the apparent induction by microwaves of heat-shock gene expression in the nematode Caenorhabditis Elegans. Bioelectromagnetics 27:88-97. https://doi.org/10.1002/bem.20192

Dayalan Naidu S, Dinkova-Kostova AT (2017) Regulation of the mammalian heat shock factor 1. FEBS J 284(11):1606-1627. https://doi.org/10.1111/febs.13999

Ennamany R, Fitoussi R, Vie K, Rambert J, De Benetti L, Djavad Mossalayi M (2008) Exposure to Electromagnetic Radiation Induces Characteristic Stress Response in Human Epidermis Journal of Investigative Dermatology 128:743-746. https://doi.org/10.1038/sj.jid.5701052

Dong, Bushu, Alex M Jaeger, Dennis J Thiele (2019) Inhibiting Heat Shock Factor 1 in Cancer: A Unique Therapeutic Opportunity. Trends in pharmacological sciences 40:986-1005. https://doi.org/10.1016/j.tips.2019.10.008

Gomez-Pastor R, Burchfiel ET, Thiele DJ (2018) Regulation of heat shock transcription factors and their roles in physiology and disease. Nat Rev Mol Cell Biol 19:4-19. https://doi.org/10.1038/nrm.2017.73

Hamdan, F. F., Y. Percherancier, B. Breton, M. Bouvier (2006) Monitoring protein-protein interactions in living cells by bioluminescence resonance energy transfer (BRET). Curr. Protoc. Neurosci. Chapter 5: Unit 5.23. https://doi.org/10.1002/0471142301.ns0523s34

Hentze N, Le Breton L, Wiesner J, Kempf G, Mayer MP (2016) Molecular mechanism of thermosensory function of human heat shock transcription factor Hsf1. Elife 5:e11576. https://doi.org/10.7554/eLife.11576

IARC Working Group on the Evaluation of Carcinogenic Risks to Humans (2013) Non-ionizing radiation, Part 2: Radiofrequency electromagnetic fields. IARC Monogr Eval Carcinog Risks Hum 102:1-460.

Kesari KK, Meena R, Nirala J, Kumar J, Verma HN (2014) Effect of 3G cell phone exposure with computer controlled 2-D stepper motor on non-thermal activation of the hsp27/p38MAPK stress pathway in rat brain. Cell Biochem Biophys 68:347-358. https://doi.org/10.1007/s12013-013-9715-4

Kim HN, Han NK, Hong MN, Chi SG, Lee YS, Kim T, Pack JK, Choi HD, Kim N, Lee JS (2012) Analysis of the cellular stress response in MCF10A cells exposed to combined radio frequency radiation. J Radiat Res 53:176-183.

Kremers GJ, Goedhart J, van Munster EB, Gadella TW (2006) Cyan and yellow super fluorescent proteins with improved brightness, protein folding, and FRET Förster radius. Biochemistry 45:6570-6580. https://doi.org/10.1021/bi0516273

Kwee S, Raskmark P, Velizarov S (2001) Changes in cellular proteins due to environmental non-ionizing radiation. I. Heat-shock proteins Electro- and Magnetobiology 20:141-152. https://doi.org/10.1081/JBC-100104139

Laszlo A, Moros EG, Davidson T, Bradbury M, Straube W, Roti Roti J (2005) The heat-shock factor is not activated in mammalian cells exposed to cellular phone frequency microwaves. Radiat Res 164:163-172. https://doi.org/10.1667/rr3406

Lee AS(2005) The ER chaperone and signaling regulator GRP78/BiP as a monitor of endoplasmic reticulum stress. Methods 35:373-381. https://doi.org/10.1016/j.ymeth.2004.10.010

Leszczynski D, Joenväärä S, Reivinen J, Kuokka R (2002) Non-thermal activation of the hsp27/p38MAPK stress pathway by mobile phone radiation in human endothelial cells: molecular mechanism for cancer- and blood-brain barrier-related effects. Differentiation 70:120-129. https://doi.org/10.1046/j.1432-0436.2002.700207.x

Li WW, Alexandre S, Cao X, Lee AS (1993) Transactivation of the grp78 promoter by Ca2+ depletion. A comparative analysis with A23187 and the endoplasmic reticulum Ca(2+)-ATPase inhibitor thapsigargin. J Biol Chem 268:12003-12009.

Lixia S, Yao K, Kaijun W, Deqiang L, Huajun H, Xiangwei G, Baohong W, Wei Z, Jianling L, Wei W (2006) Effects of 1.8 GHz radiofrequency field on DNA damage and expression of heat shock protein 70 in human lens epithelial cells. Mutat Res 602:135-142. https://doi.org/10.1016/j.mrfmmm.2006.08.010

Loening AM, Fenn TD, Wu AM, Gambhir SS (2006) Consensus guided mutagenesis of Renilla luciferase yields enhanced stability and light output. Protein Eng Des Sel 19:391-400. https://doi.org/10.1093/protein/gzl023

Loison F, Debure L, Nizard P, le Goff P, Michel D, le Dréan Y (2006) Up-regulation of the clusterin gene after proteotoxic stress: implication of HSF1-HSF2 heterocomplexes. Biochem J 395:223-231. https://doi.org/10.1042/BJ20051190

López-Furelos A, Leiro-Vidal JM, Salas-Sánchez AÁ, Ares-Pena FJ, López-Martín ME (2016) Evidence of cellular stress and caspase-3 resulting from a combined two-frequency signal in the cerebrum and cerebellum of sprague-dawley rats. Oncotarget 7:64674-64689. https://doi.org/10.18632/oncotarget.11753

López-Furelos A, Salas-Sánchez AA, Ares-Pena FJ, Leiro-Vidal JM, López-Martín E (2018) Exposure to radiation from single or combined radio frequencies provokes macrophage dysfunction in the RAW 264.7 cell line. Int J Radiat Biol 94:607-618. https://doi.org/10.1080/09553002.2018.1465610

Lucas G, Rymar VV, Du J, Mnie-Filali O, Bisgaard C, Manta S, Lambas-Senas L, Wiborg O, Haddjeri N, Piñeyro G, Sadikot AF, Debonnel G (2007) Serotonin(4) (5-HT(4)) receptor agonists are putative antidepressants with a rapid onset of action. Neuron 55:712-725. https://doi.org/10.1016/j.neuron.2007.07.041

Mathew A, Mathur SK, Jolly C, Fox SG, Kim S, Morimoto RI (2001) Stress-specific activation and repression of heat shock factors 1 and 2. Mol Cell Biol 21:7163-7171. https://doi.org/10.1128/MCB.21.21.7163-7171.2001

McNamee JP, Chauhan V (2009) Radiofrequency radiation and gene/protein expression: a review. Radiat Res 172:265-287. https://doi.org/10.1667/RR1726.1

Miyakoshi J, Takemasa K, Takashima Y, Ding GR, Hirose H, Koyama S (2005) Effects of exposure to a 1950 MHz radio frequency field on expression of Hsp70 and Hsp27 in human glioma cells. Bioelectromagnetics 26:251-257. https://doi.org/10.1002/bem.20077

Miyakoshi J, Tonomura H, Koyama S, Narita E, Shinohara N (2019) Effects of Exposure to 5.8 GHz Electromagnetic Field on Micronucleus Formation, DNA Strand Breaks, and Heat Shock Protein Expressions in Cells Derived From Human Eye. IEEE Trans Nanobioscience 18:257-260. https://doi.org/10.1109/TNB.2019.2905491

Miyawaki A, Niino Y (2015) Molecular spies for bioimaging--fluorescent protein-based probes. Mol Cell 58:632-643. https://doi.org/10.1016/j.molcel.2015.03.002

Novoselova EG, Glushkova OV, Khrenov MO, Parfenyuk SB, Lunin SM, Vinogradova EV, Novoselova TV, Fesenko EE (2017) Involvement of the p38 MAPK signaling cascade in stress response of RAW 264.7 macrophages. Dokl Biol Sci 476:203-205. https://doi.org/10.1134/S0012496617050015

Ohtani S, Ushiyama A, Maeda M, Hattori K, Kunugita N, Wang J, Ishii K (2016) Exposure time-dependent thermal effects of radiofrequency electromagnetic field exposure on the whole body of rats. J Toxicol Sci 41:655-666. https://doi.org/10.2131/jts.41.655

Percherancier Y, Berchiche YA, Slight I, Volkmer-Engert R, Tamamura H, Fujii N, Bouvier M, Heveker N (2005) Bioluminescence resonance energy transfer reveals ligand-induced conformational changes in CXCR4 homo- and heterodimers. J Biol Chem 280:9895-9903. https://doi.org/10.1074/jbc.M411151200

de Pomerai D, Daniells C, David H, Allan J, Duce I, Mutwakil M, Thomas D, Sewell P, Tattersall J, Jones D, Candido P (2000) Non-thermal heat-shock response to microwaves. Nature 405:417-418. https://doi.org/10.1038/35013144

de Pomerai DI, Smith B, Dawe A, North K, Smith T, Archer DB, Duce IR, Jones D, Candido EP (2003) Microwave radiation can alter protein conformation without bulk heating. FEBS Lett 543:93-97. https://doi.org/10.1016/s0014-5793(03)00413-7

Poque E, Arnaud-Cormos D, Patrignoni L, Ruigrok HJ, Poulletier De Gannes F, Hurtier A, Renom R, Garenne A, Lagroye I, Leveque P, Percherancier Y (2020) Effects of radiofrequency fields on RAS and ERK kinases activity in live cells using the Bioluminescence Resonance Energy Transfer technique. Int J Radiat Biol :1-8. https://doi.org/10.1080/09553002.2020.1730016

Ruigrok HJ, Arnaud-Cormos D, Hurtier A, Poque E, de Gannes FP, Ruffié G, Bonnaudin F, Lagroye I, Sojic N, Arbault S, Lévêque P, Veyret B, Percherancier Y (2018) Activation of the TRPV1 Thermoreceptor Induced by Modulated or Unmodulated 1800 MHz Radiofrequency Field Exposure. Radiat Res 189:95-103. https://doi.org/10.1667/RR14877.1

Ruigrok HJ, Shahid G, Goudeau B, Poulletier de Gannes F, Poque-Haro E, Hurtier A, Lagroye I, Vacher P, Arbault S, Sojic N, Veyret B, Percherancier Y (2017) Full-Spectral Multiplexing of Bioluminescence Resonance Energy Transfer in Three TRPV Channels. Biophys J 112:87-98. https://doi.org/10.1016/j.bpj.2016.11.3197

Sanchez S, Milochau A, Ruffie G, Poulletier de Gannes F, Lagroye I, Haro E, Surleve-Bazeille JE, Billaudel B, Lassegues M, Veyret B (2006) Human skin cell stress response to GSM-900 mobile phone signals. In vitro study on isolated primary cells and reconstructed epidermis. FEBS J 273:5491-5507. https://doi.org/10.1111/j.1742-4658.2006.05541.x

Sepehrimanesh M, Kazemipour N, Saeb M, Nazifi S (2014) Analysis of rat testicular proteome following 30-day exposure to 900 MHz electromagnetic field radiation. Electrophoresis 35:3331-3338. https://doi.org/10.1002/elps.201400273

Tabuchi, Yoshiaki, Takashi Kondo (2013) Targeting Heat Shock Transcription Factor 1 for Novel Hyperthermia Therapy. International journal of molecular medicine 32: 3-8. https://doi.org/10.3892/ijmm.2013.1367

Tian F, Nakahara T, Wake K, Taki M, Miyakoshi J (2002) Exposure to 2.45 GHz electromagnetic fields induces hsp70 at a high SAR of more than 20 W/kg but not at 5W/kg in human glioma MO54 cells. Int J Radiat Biol 78:433-440. https://doi.org/10.1080/09553000110115649

Valbonesi P, Franzellitti S, Bersani F, Contin A, Fabbri E (2014) Effects of the exposure to intermittent 1.8 GHz radio frequency electromagnetic fields on HSP70 expression and MAPK

signaling pathways in PC12 cells. Int J Radiat Biol 90:382-391. https://doi.org/10.3109/09553002.2014.892225

Vecchia P, Matthes R, Ziegelberger G, Lin J and Saunders R (2009) Exposure to high frequency electromagnetic fields, biological effects and health consequences (100 kHz-300 GHz). International Comission on Non-Ionizing Radiation Protection (ICNIRP), Oberschleissheim. https://www.emf.ethz.ch/archive/var/ICNIRP_effekte_RFReview.pdf

Watilliaux A, Edeline JM, Lévêque P, Jay TM, Mallat M (2011) Effect of exposure to 1,800 MHz electromagnetic fields on heat shock proteins and glial cells in the brain of developing rats. Neurotox Res 20:109-119. https://doi.org/10.1007/s12640-010-9225-8

Yang XS, He GL, Hao YT, Xiao Y, Chen CH, Zhang GB, Yu ZP (2012) Exposure to 2.45 GHz electromagnetic fields elicits an HSP-related stress response in rat hippocampus. Brain Res Bull 88:371-378. https://doi.org/10.1016/j.brainresbull.2012.04.002

Zhadobov M, Sauleau R, Le Coq L, Debure L, Thouroude D, Michel D, Le Dréan Y (2007) Low-power millimeter wave radiations do not alter stress-sensitive gene expression of chaperone proteins. Bioelectromagnetics. Bioelectromagnetics 28(3):188-96. https://doi.org/10.1002/bem.20285

Zou J, Guo Y, Guettouche T, Smith DF, Voellmy R (1998) Repression of heat shock transcription factor HSF1 activation by HSP90 (HSP90 complex) that forms a stress-sensitive complex with HSF1. Cell 94:471-480. https://doi.org/10.1016/s0092-8674(00)81588-3

FIGURES LEGENDS

Figure 1: Mode of action of the intermolecular HSF1 BRET assay. In the resting state, Luc-HSF1 and YFP-HSF1 co-expressed together in cells are kept under inactive monomeric forms in the cytosol mainly due to their interaction with chaperone proteins such as HSP90. As a consequence, in the resting state, HSF1-fused Luc cannot efficiently transfer its energy to HSF1-YFP. Upon proteotoxic or heat stress, chaperone proteins interact with unfolded proteins, thereby releasing HSF1 monomers that become free to interact altogether, maximising the energy transfer between Luc and YFP groups into HSF1 trimers.

Figure 2: Characterisation of the Luc-HSF1/YFP-HSF1 intermolecular BRET assay response to heat stress. A) Light emission BRET spectra of the HSF1 intermolecular BRET probe when expressed in HEK293T cells placed either at 25 °C (black circle) or 45 °C (gray circle). The light spectra of the Luc was calculated by spectral decomposition and is indicated as a dashed line. B) Evolution of the BRET signal as a function of temperature in the cell culture medium. HEK293T cells transiently co-expressing Luc-HSF1 and YFP-HSF1 proteins were heated from 22 to 47 °C using a Peltier apparatus while both BRET signal and temperature were monitored in real-time. One representative experiment out of three is presented.

Figure 3: Characterisation of Luc-HSF1/YFP-HSF1 intermolecular BRET assay response to MG132-induced proteotoxic stress. A) Dose-response curves of MG132- and thapsigargin-induced changes in Luc-HSF1/YFP-HSF1 BRET signal. HEK293T cells transiently co-expressing Luc-HSF1 and YFP-HSF1 proteins cells were activated for 12 hours at 37 °C with increasing concentration of MG132 or Thapsigargin before BRET measurement. The results represent the average ± S.E.M. of 4 (MG132) and 7 (Thapsigargin) independent experiments done in duplicate. B) Western blot analysis of BIP, HSP70 and HSF1 protein levels in cellular extract of untransfected HEK293T cells (left panel) or HEK93T cells transfected with Luc-HSF1/YFP-HSF1 (right panel), that were challenged for 12 hours with either 5 µM MG132 or 10 nM Thapsigargin. CT: No treatment. MG: MG132. TG: Thapsigargin.

Figure 4: Effects of CW 1800 MHz exposure on HSF1 activation. HEK293T cells expressing Luc-HSF1 and YFP-HSF1 were exposed to CW 1800 MHz signal at 24 W/kg, starting at 600 s, while BRET (Panel A) and temperature (Panel B) were monitored in real-time. Black circles: Temperature was allowed to rise under RF exposure; Grey squares: temperature was clamped at 35.8 °C using a Peltier apparatus; Open diamonds: control without RF exposure at 35.8 °C. One representative experiment out of three is presented.

Figure 5: Effect of RF exposure on basal and MG132-induced HSF1 activity. A-D) HEK293T cells transfected with Luc-HSF1 / YFP-HSF1 BRET probe were sham-exposed or exposed to unmodulated CW 1800 MHz (A and B), GSM-modulated 1800 MHz (C and D) or Wi-Fi-modulated 1800 MHz (E and F) signals at either 1.5 W/kg (A, C and E) or 6 W/kg (B, D and F) for 24 hours. Cells were activated using increasing concentrations of MG132 under sham or RF exposure for the last 12 h before BRET measurement. The results in panels A-F represent the average ± S.E.M. for the effect of 8 experiments performed in duplicate. G, H and I) Box and whisker plots representing the distribution of the variations of basal BRET (G), MG132-potency (H) and MG132-maximal efficacy (I) between the RF exposed- (Expo) and sham- conditions derived for each experimental conditions plotted in A-F. Statistical significance of the derivation from the null hypothesis (no difference between sham and RF exposure) was assessed using the one-Sample Wilcoxon Signed Rank Test. n.s.: not significant; *: $p<0.05$; **: $p<0.01$.

Supplementary Figure 1: Light emission spectra of Luc-HSF1 (A) and YFP-HSF1 (B). While the Luc emission spectra was acquired 5 min after the addition of coelenterazine H, the YFP emission spectra was acquired following excitation of the HEK293T transfected cells at 450 nm.

Supplementary Figure 2: Characterisation of the Luc-HSF1/YFP-HSF1 intermolecular BRET assay response to MG132-induced proteotoxic stress in HuH7 cells. A) Dose-response curves of MG132- and thapsigargin-induced changes in Luc-HSF1/YFP-HSF1 BRET signal. HuH7 cells transiently co-expressing Luc-HSF1 and YFP-HSF1 proteins cells were activated for 12 hours at 37 °C with increasing concentration of MG132 or Thapsigargin before BRET measurement. The results represent the average ± S.E.M. of 4 independent experiments done in duplicate. B) Western blot analysis of BIP, HSP70 and HSF1 protein levels in cellular extract of untransfected HuH7 cells (left panel) or HuH7 cells transfected with Luc-HSF1/YFP-HSF1 (right panel), that were challenged for 12 h with either 5 μM MG132 or 10 nM Thapsigargin. CT: No treatment. MG: MG132. TG: Thapsigargin.

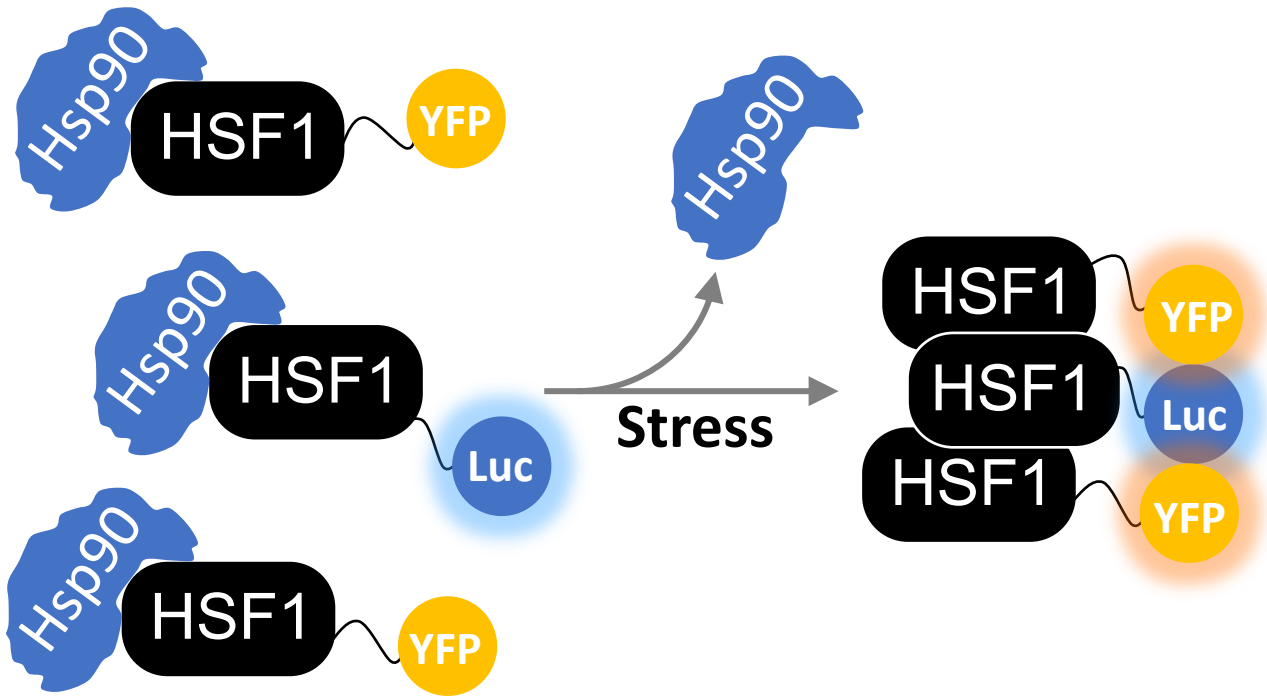
Hsp90
HSF1
YFP
Hsp90
HSF1
Luc
Hsp90
HSF1
YFP
Stress
Hsp90
HSF1
HSF1
YFP
HSF1
Luc
HSF1
YFP

Figure 1

A

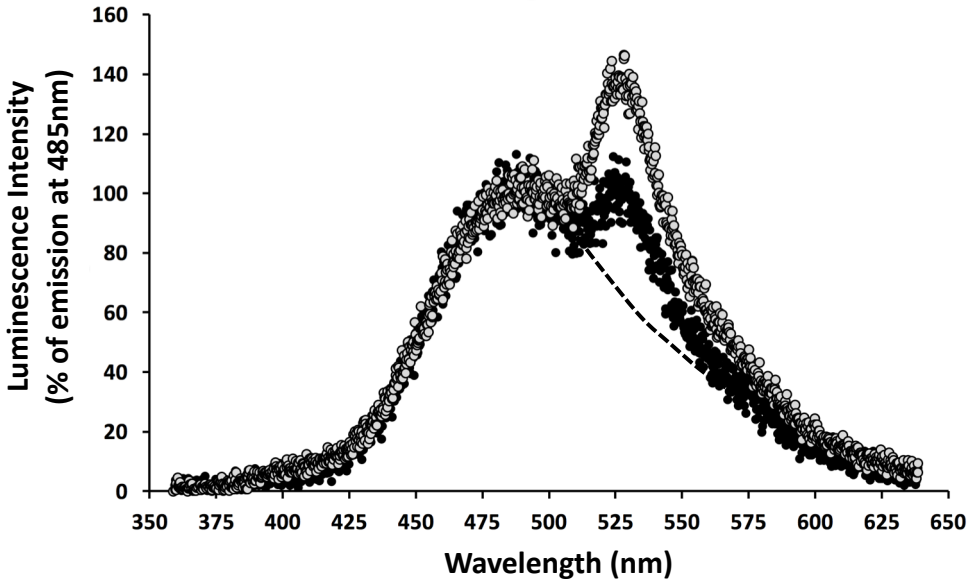
Luminescence Intensity
(% of emission at 485nm)
160
140
120
100
80
60
40
20
0
350
375
400
425
450
475
500
525
550
575
600
625
650
Wavelength (nm)

B

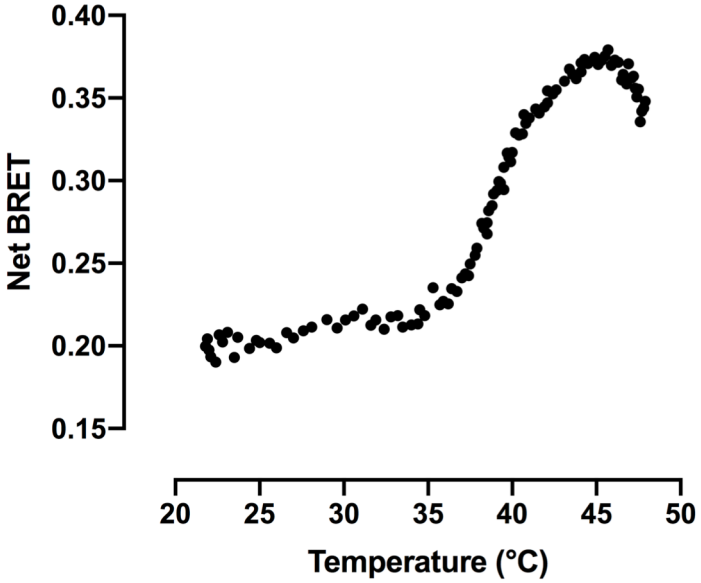
Net BRET
0.40
0.35
0.30
0.25
0.20
0.15
20
25
30
35
40
45
50
Temperature (°C)

Figure 2

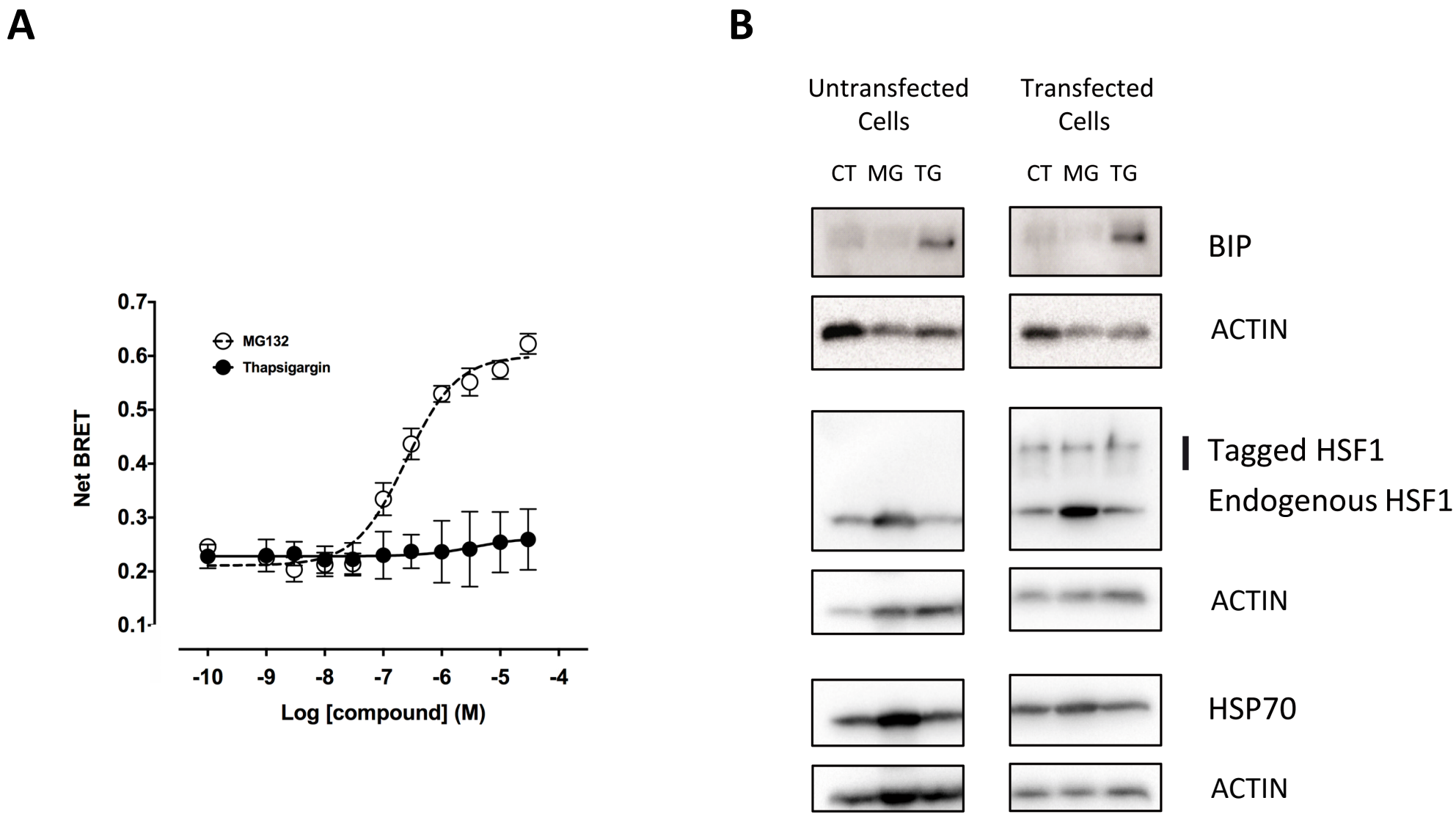
A
B
Net BRET
0.7
0.6
0.5
0.4
0.3
0.2
0.1
MG132
Thapsigargin
-10
-9
-8
-7
-6
-5
-4
Log [compound] (M)
Untransfected Cells
Transfected Cells
CT MG TG
CT MG TG
BIP
ACTIN
Tagged HSF1
Endogenous HSF1
ACTIN
HSP70
ACTIN

Figure 3

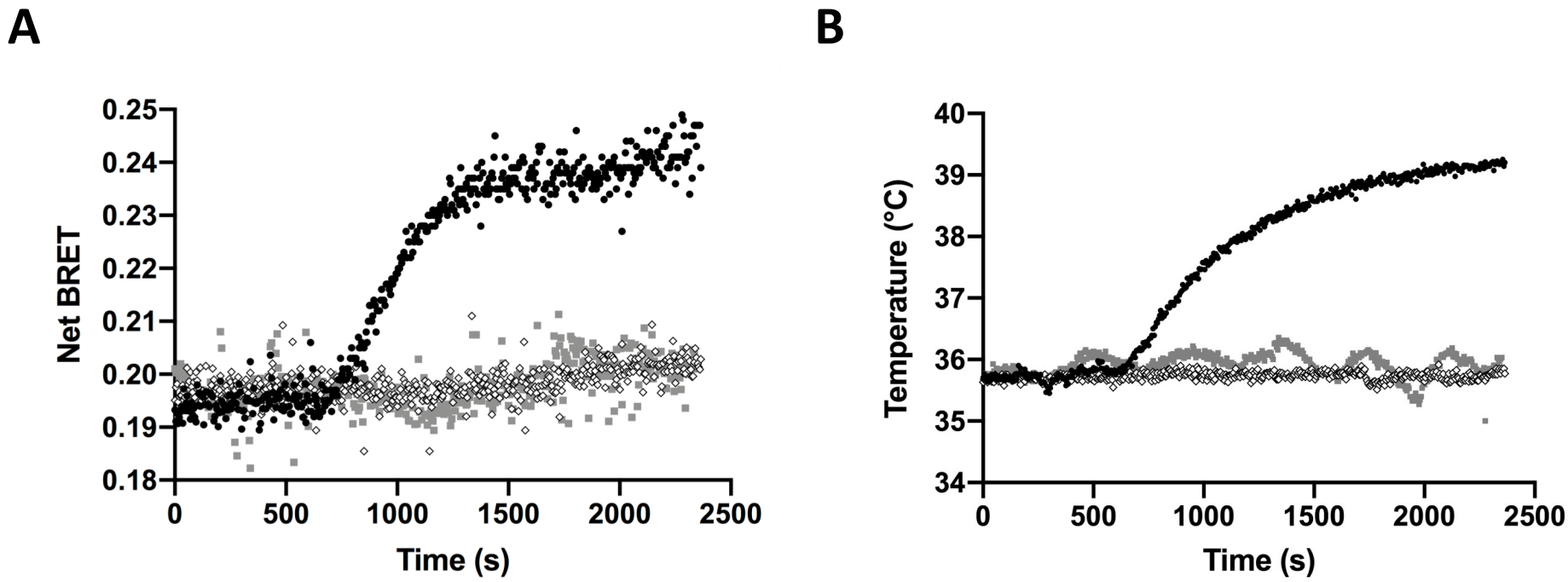
A
Net BRET
0.25
0.24
0.23
0.22
0.21
0.20
0.19
0.18
0
500
1000
1500
2000
2500
Time (s)
B
Temperature (°C)
40
39
38
37
36
35
34
0
500
1000
1500
2000
2500
Time (s)

Figure 4

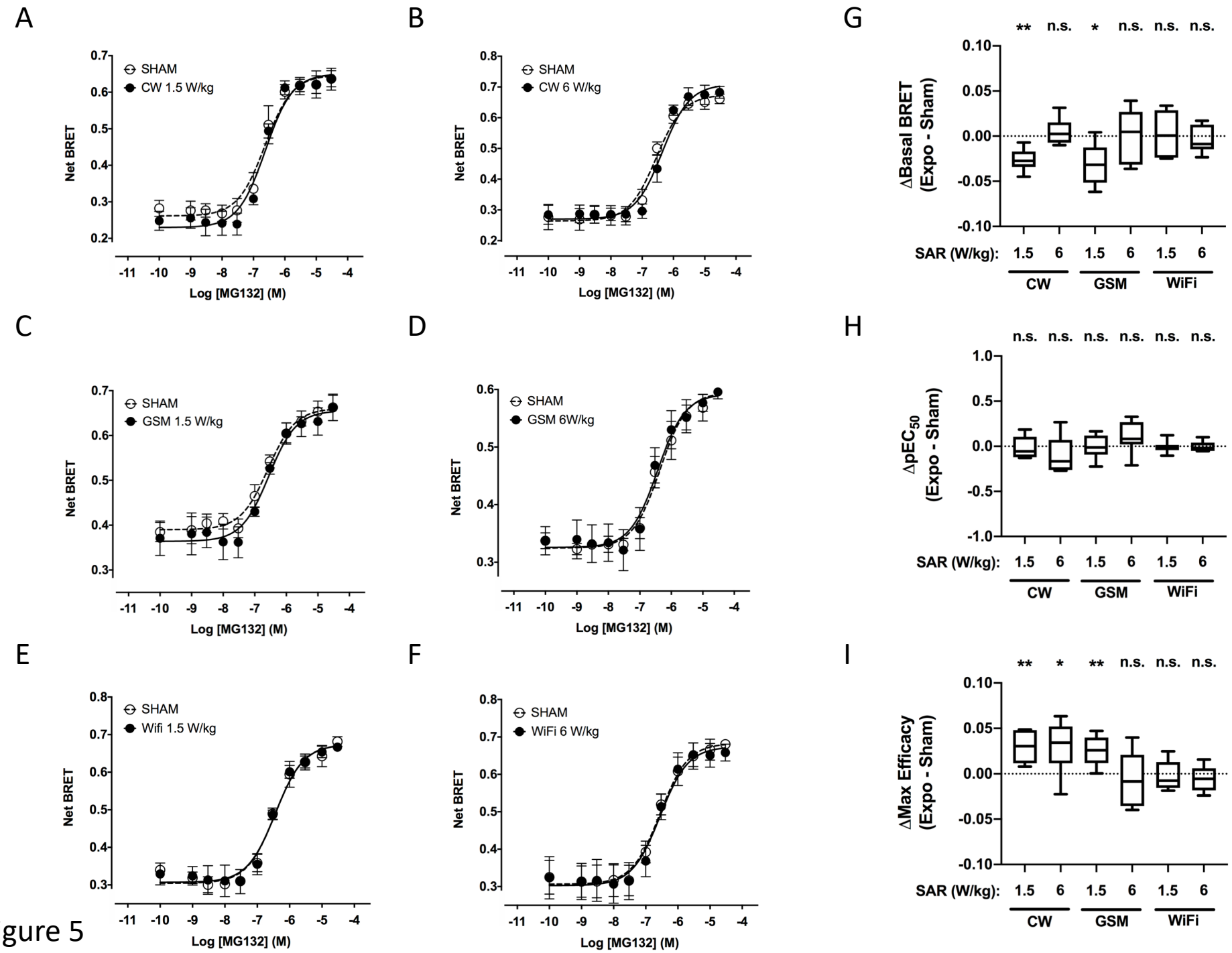
A
SHAM
CW 1.5 W/kg
Net BRET
Log [MG132] (M)
B
SHAM
CW 6 W/kg
Net BRET
Log [MG132] (M)
C
SHAM
GSM 1.5 W/kg
Net BRET
Log [MG132] (M)
D
SHAM
GSM 6W/kg
Net BRET
Log [MG132] (M)
E
SHAM
Wifi 1.5 W/kg
Net BRET
Log [MG132] (M)
F
SHAM
WiFi 6 W/kg
Net BRET
Log [MG132] (M)
G
** n.s. * n.s. n.s. n.s.
ΔBasal BRET (Expo - Sham)
SAR (W/kg): 1.5 6 1.5 6 1.5 6
CW GSM WiFi
H
n.s. n.s. n.s. n.s. n.s. n.s.
ΔpEC50 (Expo - Sham)
SAR (W/kg): 1.5 6 1.5 6 1.5 6
CW GSM WiFi
I
** * ** n.s. n.s. n.s.
ΔMax Efficacy (Expo - Sham)
SAR (W/kg): 1.5 6 1.5 6 1.5 6
CW GSM WiFi

Figure 5

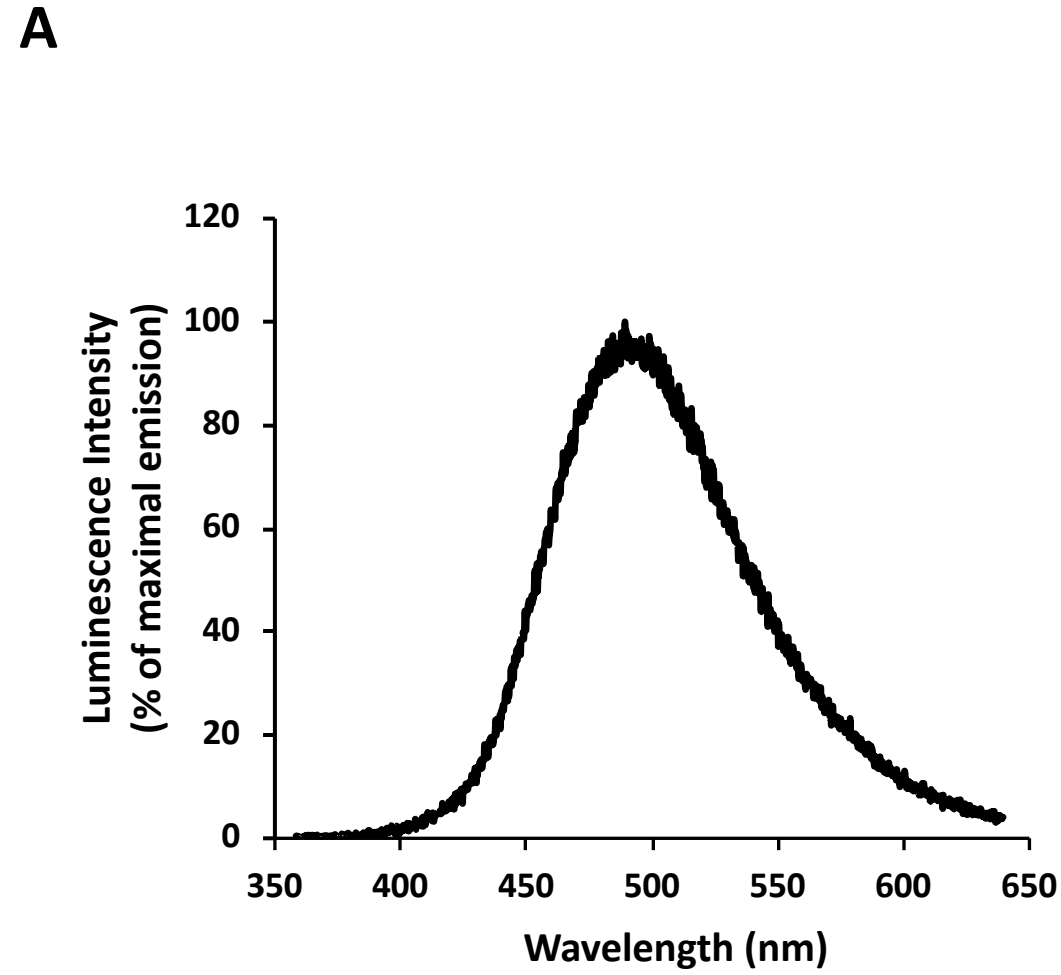

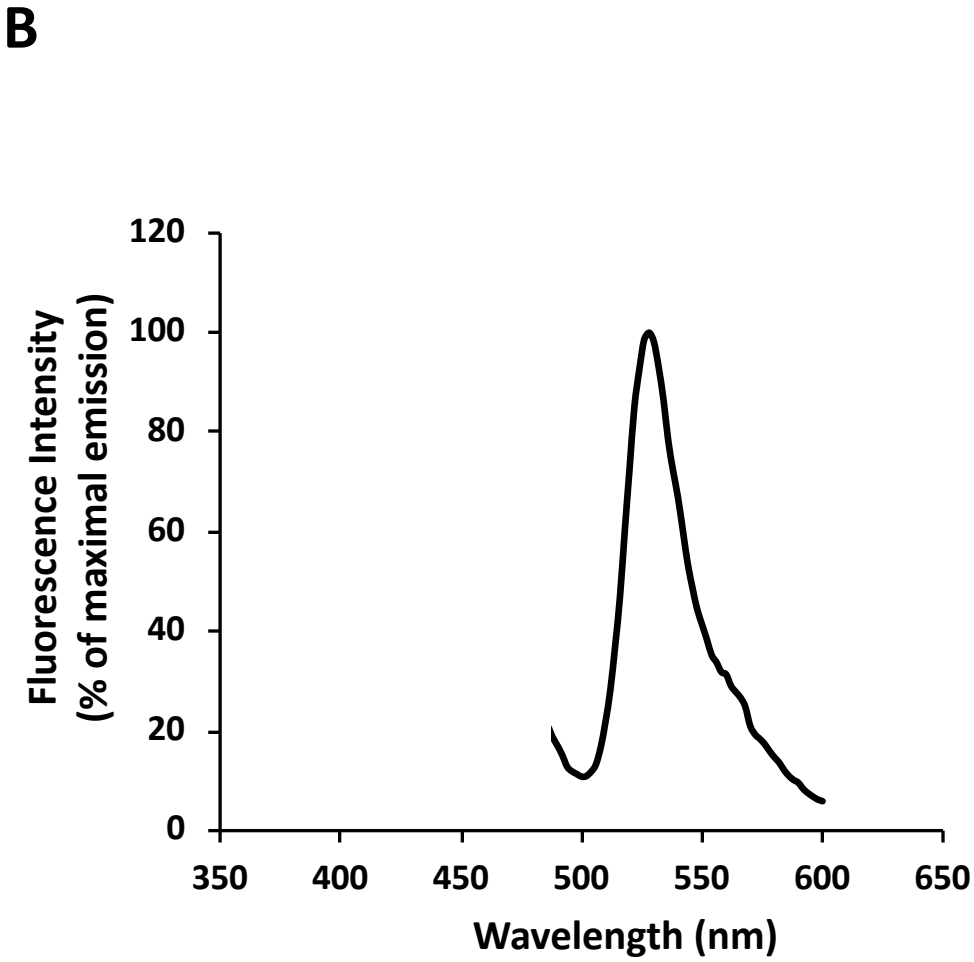

Supplementary Figure 1

A

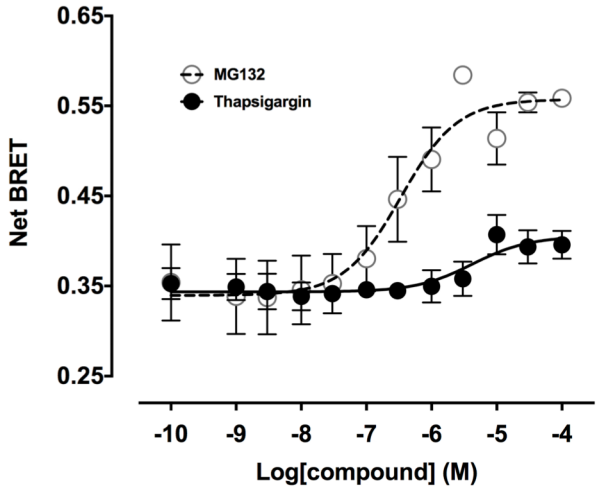

B

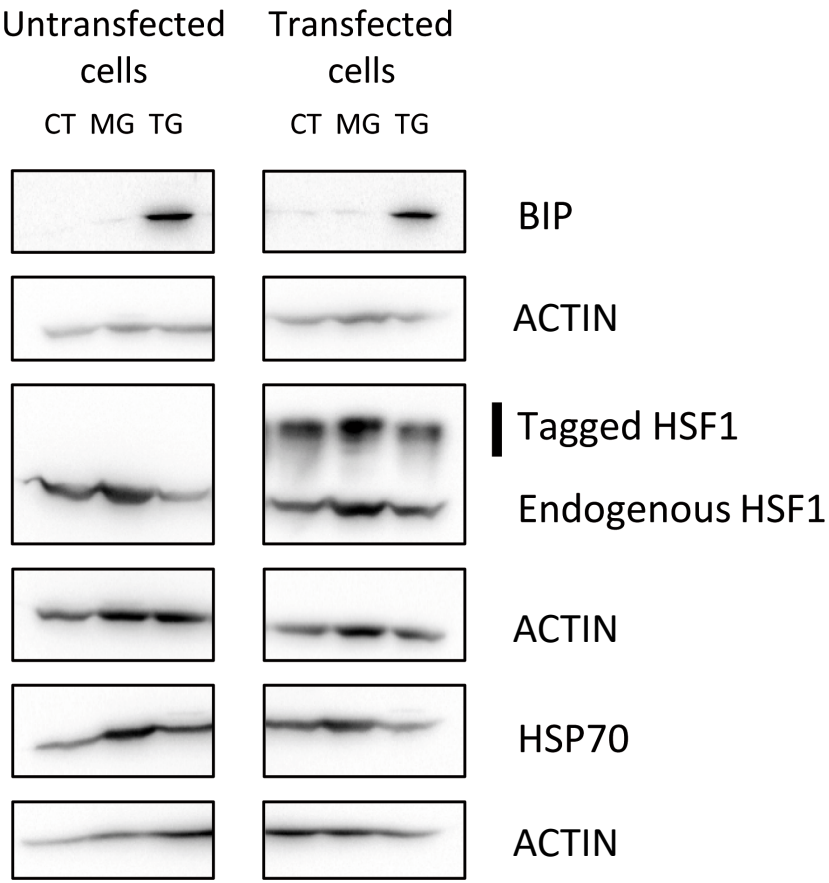

Supplementary Figure 2